Effect of cracks on the thermal resistance of aligned fiber composites

J. Dryden
Department of Mechanical and Materials Engineering, University of Western Ontario, London, Ontario N6A 5B9, Canada

A. Deakin
Department of Applied Mathematics, University of Western Ontario, London, Ontario N6A 5B9, Canada

F. Zok
Department of Materials, University of California, Santa Barbara, California 93106

(Received 18 February 2002; accepted for publication 18 April 2002)

The axial heat flow within an aligned fiber composite containing matrix cracks bridged by the fibers is analyzed. A unit cell is defined and an exact expression for the constriction resistance of the unit cell is found. For values of fiber volume fraction and crack spacing that occur in actual composites, the thermal interaction between cracks is found to be almost negligible when the fiber/matrix interface is perfect. The asymptotic behavior under conditions of severe interface debonding is found. [DOI: 10.1063/1.1486052]

I. INTRODUCTION

In an aligned fiber composite, the overall longitudinal thermal conductivity is given by the law of mixtures. After being subjected to tensile stress, the composite may develop matrix cracks which are bridged by the fibers, and this cracking causes an increase in the longitudinal thermal resistance. A commonly used method of analyzing problems of this type is to define a representative unit cell, analyze the heat flow within this test region, and then relate the properties of this cell to the overall macroscopic properties. This unit cell approach was first applied to the present situation by Lu and Hutchinson,[1] and they obtained an approximate solution for the thermal field within the unit cell. Subsequently, using the same type of cell, upper and lower bounds for the constriction resistance were obtained,[2] and it was shown that in some cases, the approximate treatment given by Lu and Hutchinson did not give accurate results. Although the aforementioned bounds are rigorous, their use is somewhat cumbersome, and the objective of the present article is to present an exact analysis for the thermal field within the unit cell.

II. PRELIMINARY CONSIDERATIONS

Figure 1 shows an idealized microstructure in which the cracks have uniform spacing, the cracks are bridged by fibers and heat flow is in the direction of the fibers. Figure 2 shows a unit cell where the fiber diameter is equal to $2a$, the distance between fiber centers is equal to $2b$, and the cell length L is equal to one half of the crack spacing. The volume fraction f of the fibers in the unit cell is

$$f \equiv \frac{a^2}{b^2}. \tag{1}$$

In a pristine specimen, i.e., if the cracks are not present, the temperature throughout the cell is given by

$$T = \frac{QL}{\pi b^2 k_z}\left\{1 - \frac{z}{L}\right\}, \tag{2}$$

where the z direction is in the fiber direction and Q is the total flux carried within the cell. The longitudinal conductivity k_z is found using the law of mixtures

$$k_z = f k_f + (1-f) k_m, \tag{3}$$

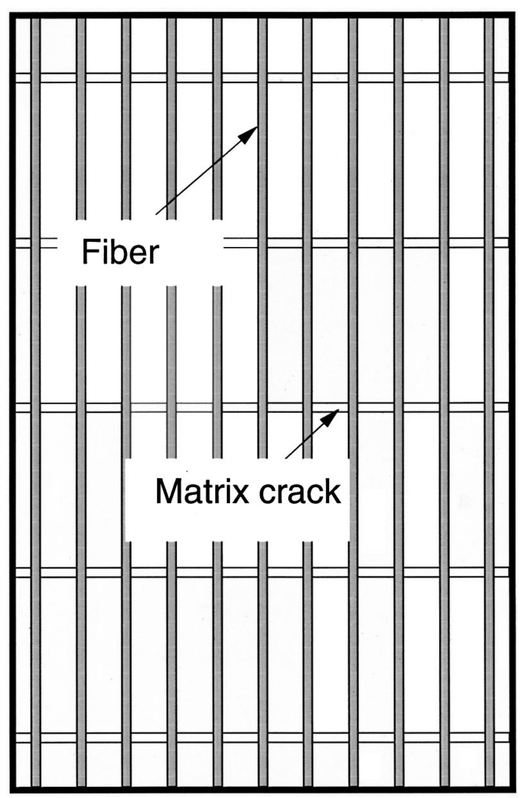

FIG. 1. Schematic of the aligned fiber composite showing the matrix cracks that are bridged by the fibers. The distance between cracks is $2L$.

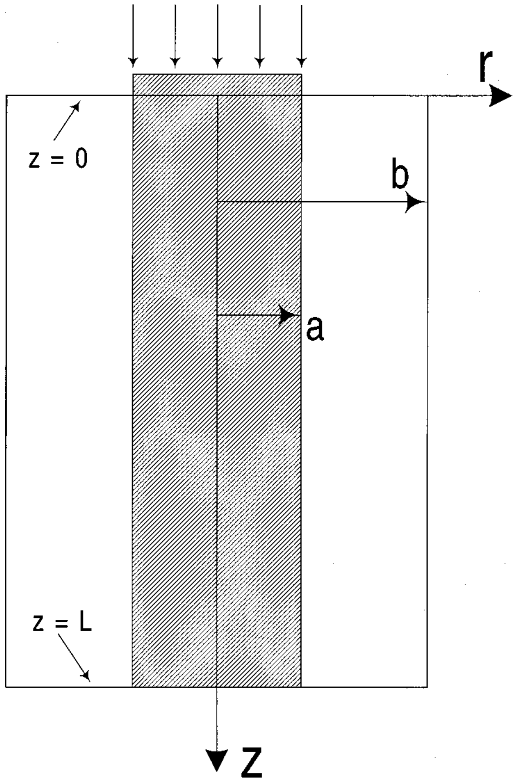

FIG. 2. The unit cell showing uniform axial flux entering across the bridging fiber. The fiber diameter is $2a$, the distance between fiber centers is $2b$, and L is the length of the cell; two cells comprise a repeating unit.

where k_m and k_f represent the thermal conductivities of the matrix and the fiber, respectively. The thermal resistance of a pristine unit cell is

$$R_0=\frac{L}{\pi b^2 k_z}. \tag{4}$$

The presence of the cracks disturb this uniform flow. The resistance R of the damaged cell is somewhat larger

$$R=R_0+R_d, \tag{5}$$

where R_d is the extra resistance due to the damage. The constriction resistance R_C and the resistance R_G of the gas represent parallel heat flow paths. It has been shown previously[2] that

$$\frac{1}{R_d}=\frac{1}{R_C}+\frac{1}{R_G}, \tag{6}$$

where

$$R_G=\frac{(1-f)fk_m^2}{2\pi a^2 h_c k_z^2}, \tag{7}$$

and h_c is the crack conductance. In Eq. (5), the constriction resistance R_C is the only unknown quantity and the analysis thus focuses solely on this quantity.

III. THERMAL FIELD WITHIN THE SOLID

As shown in Fig. 2, all of the heat enters the cell across the bridging fiber. The crack opening $2\delta L$ is assumed to be sufficiently small so that the thermal resistance, $\delta L/\pi a^2 k_f$, of the fiber bridge is negligible, and the extra thermal resistance of the unit cell is equal to the constriction resistance R_C.

After the cracks develop, the expressions for the temperatures, in the fiber and matrix, become more complicated than the simple expression in Eq. (2). The fiber and matrix temperatures are written as

$$T_f(r,z)=\frac{QL}{\pi b^2 k_z}\left\{1-\frac{z}{L}+U(r,z)\right\},$$

$$T_m(r,z)=\frac{QL}{\pi b^2 k_z}\left\{1-\frac{z}{L}+V(r,z)\right\}. \tag{8}$$

The unknown functions, $U=U(r,z)$ and $V=V(r,z)$, which describe the perturbation of the heat flow due to the constriction, are to be found. The imposed flux boundary condition on the axial heat flux entering the solid at $z=0$ is

$$\left.\frac{\partial T_f}{\partial z}\right|_0=-\frac{Q}{\pi a^2 k_f}\rightarrow\left.\frac{\partial U}{\partial z}\right|_0=-\frac{1}{L}\frac{(1-f)k_m}{fk_f},$$

$$\left.\frac{\partial T_m}{\partial z}\right|_0=0\rightarrow\left.\frac{\partial V}{\partial z}\right|_0=\frac{1}{L}. \tag{9}$$

At the other end of the cell, the isothermal plane CD in Fig. 2 corresponds to $z=L$ and, with no loss in generality, the temperature on CD can be taken as zero

$$T_f(r,L)=T_m(r,L)=0\rightarrow U(r,L)=V(r,L)=0. \tag{10}$$

Along the length of the fiber, at the interface $r=a$, the two boundary conditions

$$k_f\left.\frac{\partial U}{\partial r}\right|_a=k_m\left.\frac{\partial V}{\partial r}\right|_a,$$

$$k_f\left.\frac{\partial U}{\partial r}\right|_a=h[V(a)-U(a)], \tag{11}$$

must be satisfied. The first condition is a radial flux balance, while the second condition relates the temperature jump, $V(a)-U(a)$, to the flux. The adiabatic condition at $r=b$ requires that

$$k_m\left.\frac{\partial V}{\partial r}\right|_b=0. \tag{12}$$

Series solution for $U(r,z)$ and $V(r,z)$

In the axisymmetric coordinate system used here, the Laplacian operator ∇^2 is expressed as

$$\nabla^2\equiv\frac{\partial^2}{\partial r^2}+\frac{1}{r}\frac{\partial}{\partial r}+\frac{\partial^2}{\partial z^2}, \tag{13}$$

and the two harmonic functions must satisfy $\nabla^2 U=\nabla^2 V=0$. The problem then is to find the two harmonic functions, U and V, which satisfy the boundary conditions just described.

To begin the analysis, the following results can be readily verified using integration by parts

$$\int_0^L \frac{\partial^2 U}{\partial z^2}\cos\alpha_n z\ dz = -\left.\frac{\partial U}{\partial z}\right|_0 - \alpha_n^2\int_0^L U\cos\alpha_n z\ dz,$$

$$\int_0^L \frac{\partial^2 V}{\partial z^2}\cos\alpha_n z\ dz = -\left.\frac{\partial V}{\partial z}\right|_0 - \alpha_n^2\int_0^L V\cos\alpha_n z\ dz, \quad (14)$$

where the eigenvalues

$$\alpha_n = \frac{\pi(2n-1)}{2L} \quad (15)$$

are chosen so that $\cos\alpha_n L = 0$. Using these results, along with the definition of ∇^2 in Eq. (13), leads to

$$\int_0^L \nabla^2 U\cos\alpha_n z\ dz = \int_0^L\left\{\frac{\partial^2 U}{\partial r^2}+\frac{1}{r}\frac{\partial U}{\partial r}-\alpha_n^2 U\right\}\cos\alpha_n z\ dz - \left.\frac{\partial U}{\partial z}\right|_0 = 0,$$

$$\int_0^L \nabla^2 V\cos\alpha_n z\ dz = \int_0^L\left\{\frac{\partial^2 V}{\partial r^2}+\frac{1}{r}\frac{\partial V}{\partial r}-\alpha_n^2 V\right\}\cos\alpha_n z\ dz - \left.\frac{\partial V}{\partial z}\right|_0 = 0. \quad (16)$$

Now, if the two functions U and V are written in series form

$$U(r,z) = \frac{2}{L}\sum_1^\infty A_n(r)\cos\alpha_n z,$$

$$V(r,z) = \frac{2}{L}\sum_1^\infty B_n(r)\cos\alpha_n z, \quad (17)$$

and if these series are subsequently substituted in Eq. (16), then due to the orthogonality properties of the cosine functions, the following two ordinary differential equations are obtained:

$$\frac{d^2 A_n}{dr^2}+\frac{1}{r}\frac{dA_n}{dr}-\alpha_n^2 A_n - \left.\frac{\partial U}{\partial z}\right|_0 = 0,$$

$$\frac{d^2 B_n}{dr^2}+\frac{1}{r}\frac{dB_n}{dr}-\alpha_n^2 B_n - \left.\frac{\partial V}{\partial z}\right|_0 = 0. \quad (18)$$

In each of these two differential equations, the homogeneous solution is a modified Bessel function of order zero, and the particular solution is a constant. The function A_n must be finite at $r=0$ and the function B_n must satisfy the adiabatic condition at $r=b$. The two functions A_n and B_n are coupled by the fiber/matrix interface conditions in Eq. (11) which hold at $r=a$. The solution which satisfies these conditions is

$$A_n(r) = \frac{1}{\alpha_n^2\lambda_a}\left\{\frac{(1-f)k_m}{fk_f} - \frac{k_z\Psi_n(\alpha_n r)}{\gamma_n f k_f}\right\},$$

$$B_n(r) = -\frac{1}{\alpha_n^2\lambda a}\left\{1-\frac{k_z\Omega_n(\alpha_n r)}{\gamma_n f k_m}\right\}. \quad (19)$$

The functions $\Psi_n(\alpha_n r)$ and $\Omega_n(\alpha_n r)$ are defined in terms of the modified Bessel functions $I_n(x)$ and $K_n(x)$ as

$$\Psi_n(\alpha_n r) = \frac{I_0(\alpha_n r)}{I_1(\xi_n)},$$

$$\Omega_n(\alpha_n r) = \frac{I_1(\mu_n)K_0(\alpha_n r)+I_0(\alpha_n r)K_1(\mu_n)}{I_1(\mu_n)K_1(\xi_n)-I_1(\xi_n)K_1(\mu_n)}, \quad (20)$$

and the various dimensionless coefficients are

$$\kappa = k_f/k_m, \quad \rho = k_f/ah, \quad \lambda = L/a, \quad \xi_n = a\alpha_n,$$

$$\mu_n = b\alpha_n, \quad \gamma_n = \Psi_n(\xi_n)+\kappa\Omega(\xi_n)+\rho\xi_n. \quad (21)$$

Finally, by substituting the expressions for A_n and B_n into the series, then using the known expansion, $2\Sigma_1^\infty \cos\alpha_n z/\alpha_n^2 = L(L-z)$, the functions U and V are found as

$$U(r,z) = \frac{(1-f)k_m}{fk_f}\left\{1-\frac{z}{L}\right\} - \frac{2k_z}{\lambda^2 f k_f}\sum_1^\infty \frac{\Psi_n(\alpha_n r)\cos(\alpha_n z)}{\gamma_n\xi_n^2},$$

$$V(r,z) = \left\{\frac{z}{L}-1\right\} + \frac{2k_z}{\lambda^2 f k_m}\sum_1^\infty \frac{\Omega_n(\alpha_n r)\cos(\alpha_n z)}{\gamma_n\xi_n^2}. \quad (22)$$

Considering the expression for $U(r,z)$, the linear profile along the length, given in the first term in Eq. (22), represents the temperature in the case where the fiber is completely decoupled from the matrix, i.e., in the absence of radial diffusion across the fiber/matrix interface. The second term, involving the infinite sum, accounts for the thermal coupling across the interface. A similar interpretation applies to the matrix term $V(r,z)$.

IV. CONSTRICTION RESISTANCE

The constriction resistance is defined as $R_C \equiv \overline{\Delta T_f}/Q$, where $\overline{\Delta T_f}$ is the *extra* average temperature rise across the fiber caused by constriction. Using Eqs. (8) and (22), the constriction resistance can be evaluated:

$$R_C \equiv \frac{\overline{\Delta T_f}}{Q} = \frac{2\pi Q R_L}{Q\pi a^2}\int_0^a U(r,0)r\ dr,$$

$$= \mathcal{R}_C\Phi. \quad (23)$$

The quantity $\mathcal{R}_C$ represents the constriction resistance of heat flowing into a semi-infinite solid, see for example Carslaw and Jaeger,[3] and is written as

$$\mathcal{R}_C = \frac{8}{3\pi^2 a k_f}.$$

The heat flows uniformly through a spot of radius "a" into the semi-infinite solid with conductivity k_f. The constriction resistance factor Φ, appearing in Eq. (23), accounts for the effects of both inhomogeneity and the finite geometry of the cell. Its use was suggested by Cooper *et al.*[4] and it was applied to uniform solids.

The constriction resistance factor (CRF) is written in the form

$$\Phi = \zeta\lambda - \theta, \quad (24)$$

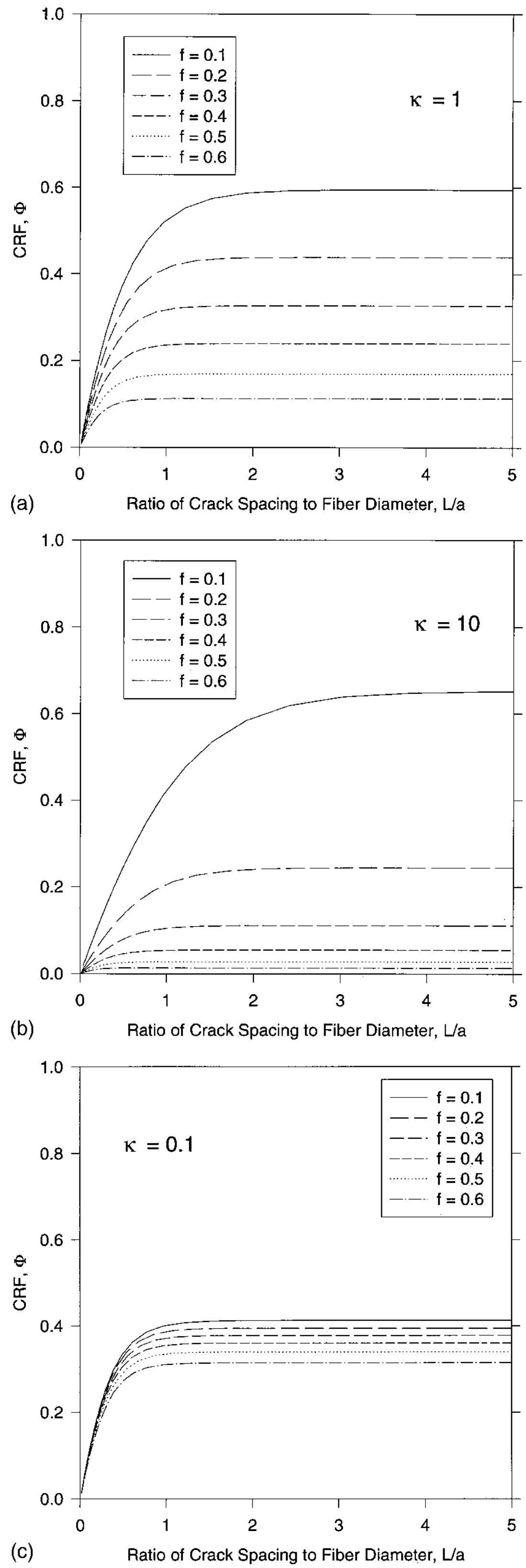

FIG. 3. The constriction resistance factor Φ as a function of the crack spacing λ evaluated for various values of the volume fraction *f*. The following values of the conductivity ratio are used: (a) $\kappa=1$, (b) $\kappa=10$, and (c) $\kappa=0.1$.

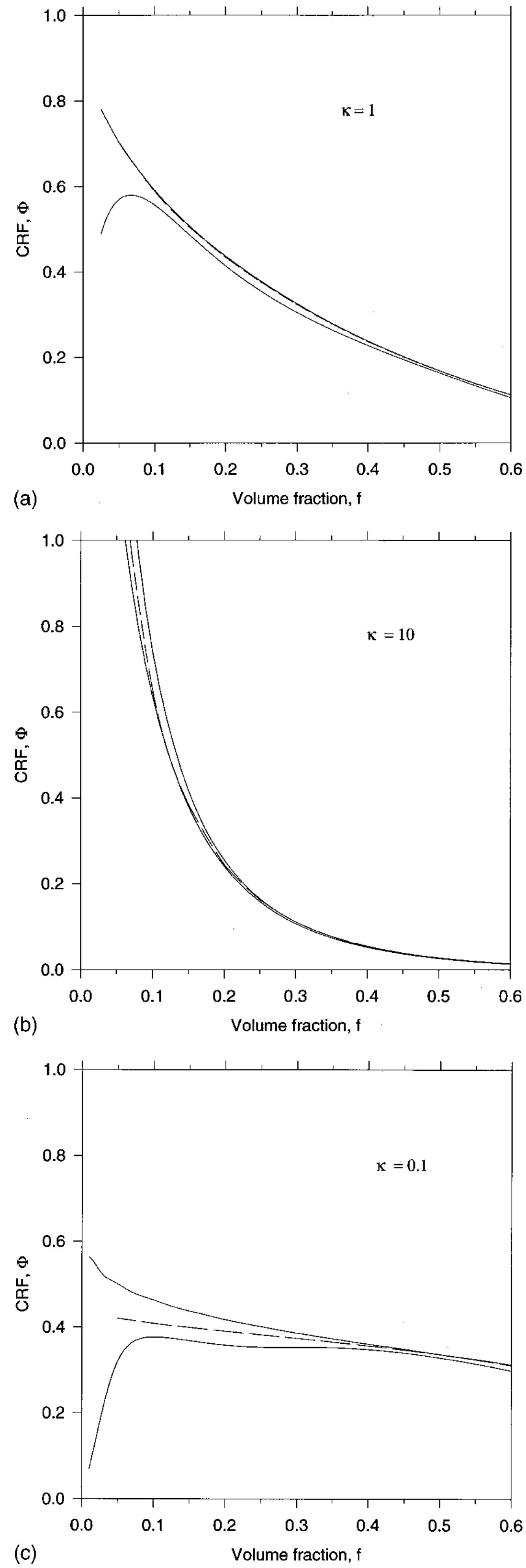

FIG. 4. Comparison between the exact solution, evaluated at $\lambda=5$, against the upper and lower bounds previously obtained. The dotted line shows the exact solution and the solid lines show the bounds. The following values of the conductivity ratio are used: (a) $\kappa=1$, (b) $\kappa=10$, and in (c) $\kappa=0.1$. In (a), the upper bound represents the exact solution when $\lambda\rightarrow\infty$, and the dotted line is almost indistinguishable.

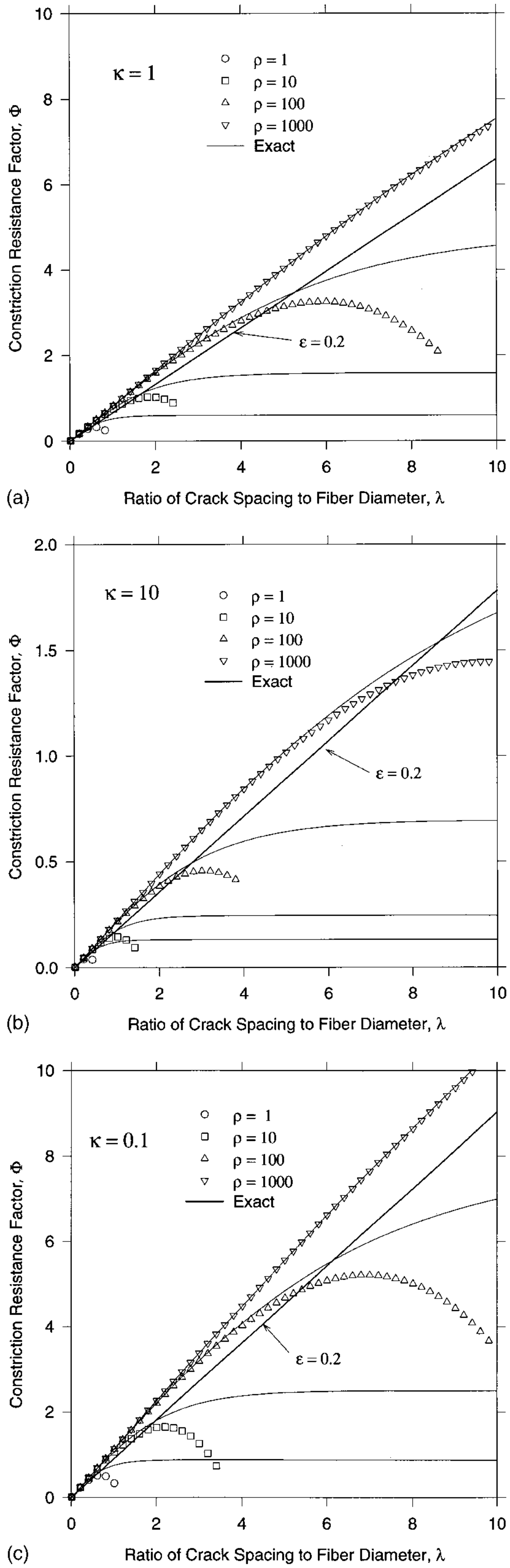

FIG. 5. The behavior of the exact solution, Φ, and the debonded approximation, Φ_d, as a function of the normalized crack spacing λ. In these figures, the volume fraction is $f=0.3$, and the following values for κ used: (a) $\kappa=1$, (b) $\kappa=1$, and in (c) $\kappa=0.1$. Each of the symbols represent a different value of ρ as shown. The heavy solid line, $\Phi=0.8\zeta\lambda$, is found by setting $\epsilon=0.2$ in Eq. (27) and Φ_d gives a useful estimate for the CRF when $\phi_d>0.8\zeta\lambda$.

where ζ and θ are given by

$$\zeta=\frac{3\pi(1-f)k_m}{8k_z},$$

$$\theta=\frac{12\lambda^2}{\pi^2}\sum_1^{\infty}\frac{1}{\gamma_n(2n-1)^3}. \qquad (25)$$

When the crack spacing λ becomes sufficiently large, the expression for Φ approaches a constant value which is independent of λ. Finally, it should be stated that the convergence of the infinite series becomes slow when the ratio $\lambda \gg 1$, and in fact the series goes over to an infinite integral.

A. Perfect interface

When the interface is thermally perfect, the dimensionless resistance $\rho=0$. The behavior of Φ as a function of λ is shown for values of $\kappa=1$, 10, 0.1 in Figs. 3(a), 3(b), and 3(c). The various curves in Figs. 3(a)–3(c) correspond to values $f=0.1$ to 0.6. The thermal interaction between cracks diminishes as λ becomes large and, for all intents, the CRF approaches a constant value when $\lambda \geqslant 2$.

In practical cases, the crack spacing is almost always greater than twice the fiber diameter and a value of $\lambda \approx 5$ is fairly typical. For these large values of λ, there is virtually no thermal interaction between the cracks. The behavior where there is no thermal interaction has been previously investigated,[2] and bounds on the CRF were obtained. Figs. 4(a)–4(c) compare the exact value of Φ, as a function of volume fraction f, against these bounds. Values of $\kappa=1$, 10, and 0.1 are used and the exact value falls between the bounds.

B. Debonded interface

According to Eq. (21) the term $\gamma_n=\Psi_n(\xi_n)+\kappa\Omega(\xi_n)+\rho\xi_n$, and if the interface debonding is severe the resistance ρ becomes large so that $\gamma_m \sim \rho\xi_n$. The summation for θ can then be found as a closed form

$$\theta \approx \frac{12\lambda^2}{\rho\pi^2}\sum_1^{\infty}\frac{1}{\xi_n(2n-1)^3}=\frac{24\lambda^3}{\rho\pi^3}\sum_1^{\infty}\frac{1}{(2n-1)^4}=\frac{\pi\lambda^3}{4\rho}.$$

Therefore, the constriction resistance factor describing this debonded behavior is labeled Φ_d and is written as

$$\Phi_d=\zeta\lambda-\frac{\pi\lambda^3}{4\rho}, \qquad (26)$$

where the subscript "d" indicates the debonded behavior. Inherent in this approximation is assumption that the amount of radial diffusion is small and most of the flux is carried by the fiber. The axial resistance of the fiber is $R_f=L/\pi a^2 k_f$ and $R_i=1/2\pi aLh$ is the resistance to radial flow due to the interface. The ratio of these two resistance is $R_f/R_i=2\lambda^2/\rho$, and for a sufficiently small values of R_f/R_i there is little radial heat flow. It seems reasonable that the region of validity for the approximate debonded model can be expressed as

$$\Phi_d \geqslant \lambda\zeta(1-\epsilon), \qquad (27)$$

where $\epsilon=\pi\lambda^2/4\zeta\rho=\pi(R_i/R_f)/8$, and as subsequently shown, using a value $\epsilon=0.2$ gives reasonable results.

For a given volume fraction, $f=0.3$, a comparison between the exact value Φ and debonded approximation Φ_d is made. This comparison is shown, for $\kappa=1$ in Fig. 5(a), for $\kappa=19$ in Fig. 5(b), and for $\kappa=0.1$ in Fig 5(c). In each of Figs. 5(a)–5(c), interface resistances $\rho=1$, 10, 100, and 1000 are used. The heavy line, $\Phi=0.8\zeta\lambda$, is obtained by setting $\epsilon=0.2$ in Eq. (27), and this limit line seems to give a reasonable estimate for the region of validity. For large values of ρ, the decay length $\lambda\propto\sqrt{\rho}$ and for large values of ρ the cracks interact thermally for values of $\lambda\approx5$.

V. CONCLUDING REMARKS

The thermal behavior of the aligned fiber composite containing matrix cracks has been analyzed by assuming that the damage is spatially periodic. A unit cell has been defined and an exact expression for the constriction resistance due to the presence of the crack has been found. Based on this analysis the following conclusions have been drawn:

(1) When the interface is perfect, the decay length $\lambda\approx2$. In practice, the ratio of crack spacing to fiber diameter is greater than five so there is virtually no thermal interaction between the cracks;

(2) Upon setting $\lambda=5$, the exact solution, in the case of a perfect interface, falls almost midway between the previously derived bounds;[2] and

(3) In the case wherein the interface is severely debonded, an approximate solution has been derived and this approximation can be used when $\Phi_d>0.8\zeta\lambda$.

ACKNOWLEDGMENT

Funding for this project was provided by the Natural Sciences and Engineering Research Council of Canada.

[1] T. J. Lu and J. W. Hutchison, Philos. Trans. R. Soc. London, Ser. A **351**, 595 (1995).
[2] J. Dryden and F. Zok, J. Appl. Phys. **89**, 4599 (2001).
[3] H. S. Carslaw and J. C. Jaeger, *Conduction of Heat in Solids*, 2nd ed. (Oxford University Press, Oxford, 1959), p. 216.
[4] M. G. Cooper, B. B. Mikic, and M. M. Yovanovich, Int. J. Heat Mass Transf. **12**, 279 (1969).